

Numerical simulations of convergent-divergent nozzle and straight cylindrical supersonic diffuser

R.C. Mehta^{*1} and G. Natarajan^{2a}

¹Department of Aeronautical Engineering, Noorul Islam University, Kumaracoil, 629180, Tamil Nadu, India

²Department of Mechanical Civil Engineering, Kumaracoil, 629180, Tamil Nadu, India

(Received April 15, 2014, Revised May 8, 2014, Accepted May 12, 2014)

Abstract. The flowfields inside a contour and a conical nozzle exhausting into a straight cylindrical supersonic diffuser are computed by solving numerically axisymmetric turbulent compressible Navier-Stokes equations for stagnation to ambient pressure ratios in the range 20 to 34. The diffuser inlet-to-nozzle throat area ratio and exit-to-throat area ratio are 21.77, and length-to-diameter ratio of the diffuser is 5. The flow characteristics of the conical and contour nozzle are compared with the help of velocity vector and Mach contour plots. The variations of Mach number along the centre line and wall of the conical nozzle, contour nozzle and the straight supersonic diffuser indicate the location of the shock and flow characteristics. The main aim of the present analysis is to delineate the flowfields of conical and contour nozzles operating under identical conditions and exhausting into a straight cylindrical supersonic diffuser.

Keywords: CFD simulation; supersonic diffuser; compressible flow; nozzle

1. Introduction

Flow through a convergent-divergent conical nozzle is customarily analyzed using a quasi-one-dimensional isentropic flow equation (Liepmann and Roshko 2007). The method of characteristics (Shapiro 1953) in conjunction with the Prandtl-Meyer function and isentropic relation is usually employed to design a two-dimensional contour nozzle for obtaining uniform flow at the nozzle exit and minimum nozzle length. From these studies, it is found that the location and the shape of the hump on the centre line Mach number distribution are functions of the geometrical parameters of the nozzle such as semi-cone angle of the divergent section of the nozzle (Delussu and Talice 2002). The flow separation inside the nozzle has been the subject of experimental (Frey and Hagemann 2000) theoretical (Summerfield *et al.* 1954) and numerical (Mehta *et al.* 2012) studies. The flow-field features inside the high expansion rocket nozzle are required for the optimum thrust at high altitude.

A constant area supersonic exhaust diffuser (SED) is generally used for testing the propulsive nozzles. The straight cylindrical SED can simulate low pressure environment for evaluating steady-state performance of a rocket nozzle. Massier and Roschke (1960) have conducted

*Corresponding author, Professor, E-mail: drakhab.mehta@gmail.com

^aPh.D.

experimental studies to find out the influence of SED configuration on pressure recovery. Park *et al.* (2008) made a small-scale HAT facility to evaluate the flowfield of various types of SED. A lab-scale high-altitude simulator (Yeom *et al.* 2009, Sung *et al.* 2010) was set-up to analyze the complex flowfield of the SED performance in conjunction with the experimental and the numerical methods. Sivo *et al.* (1960) describe the use of the various types of SED for the High Altitude Test facility. The challenging task in designing such a diffuser is to keep the facility length shorter and starting pressure ratio as low as possible. Goethert (1962) has carried out experimental investigation using SED. Their experimental studies have revealed that the starting stagnation pressure for a diffuser is a function of the geometrical parameters and the operating conditions of the rocket motor.

Park *et al.* (2008) investigated fluid dynamics of starting and terminating transients of ejector. Kim *et al.* (2008) have carried out analytical studies for starting pressure of an annular injection supersonic ejector. Optimization of second throat ejectors for high altitude test facilities has been numerically carried out by Kumaran *et al.* (2009). Park *et al.* (2012) investigated the nozzle expansion ratio and nozzle contour on the starting of exhaust diffuser for altitude simulation.

The flowfield features inside the nozzle and the SED are complex and difficult to visualize experimentally. The satisfactory running of the SED needs a number of pressure measurements in order to evaluate its performance. The main aim of the present work is to investigate the flow characteristics of the rocket nozzle as well as the diffuser at different stagnation-to ambient pressure ratios. The numerical simulation will help to delineate the flowfield features such as shock wave structure, separated flow regions, boundary layer growth, and static pressure variations along the centre line and wall of the straight cylindrical SED. The Reynolds-averaged Navier-Stokes (RANS) equations are used with a low Reynolds number turbulence model (Spalart and Allmaras 1992) and are solved using FLUENT (2010) flow solver. The value of $L/D=5$ is minimum length to diameter ratio for starting SED (Annamalai *et al.* 2002). Flowfield features of nozzle are obtained for the area ratio of nozzle exit to throat A_e/A^* and the area ratio of diffuser to throat A_D/A^* of 21.77.

2. Numerical analysis

The axisymmetric time-dependent compressible turbulent Reynolds-Averaged Navier-Stokes equations considered in the present analysis are in strong conservation form and are solved using the FLUENT (2010) software. The one-equation turbulence model proposed by Spalart-Allmaras (1992) is employed to compute eddy viscosity.

The following initial and boundary conditions are applied in the numerical analysis for the compressible and viscous flow inside the SED. At the nozzle wall, a no-slip condition is enforced together with adiabatic wall condition. The stagnation temperature of the air is kept at 300 K. The stagnation pressure at the nozzle inlet is varied in the range 10.0×10^5 – 17.0×10^5 Pa. The ambient pressure at the diffuser is 0.5×10^5 Pa. The axial velocity is extrapolated and the radial velocity is calculated using the inlet condition. At the centre line of the axisymmetric convergent-divergent nozzle and the straight cylindrical supersonic diffuser, the symmetric conditions are prescribed. The turbulent kinematic viscosity is set to zero at the wall.

3. Nozzle and SED geometry

The axisymmetric conical nozzle has a convergent angle 30 deg and throat diameter $D^*=0.03$ m. The semi-cone angle of the divergent section of the nozzle α is 16.557 deg. The nozzle exit diameter is $D_e=0.14$ m and is located at 0.185 m from the nozzle throat. The contour and the conical nozzles are having identical throat and the exit diameters. The maximum difference between the area ratios of the contour and the conical nozzles (Mehta *et al.* 2012) is seen at about $x=0.1$ m, where x is measured from the nozzle throat. The contour and the conical nozzles are shown in Fig. 1.

The length and diameter of the SED is 0.7 m and 0.14 m, respectively. The diameter of the SED D_D is equal to the diameter of nozzle exit D_e . The area ratio of the nozzle exit-to-throat and the area ratio of diffuser diameter-to-nozzle throat is 21.7. Geometrical detail of the SED is shown in Fig. 1.

4. Computational grid

The computational grid of SED is generated using Gambit version-2.1, and the governing fluid dynamics equations are solved using FLUENT-6.2, a finite volume based commercial CFD flow solver (FLUENT 2010). A fully coupled implicit compressible flow solver with Spalart and Allmaras (1992) turbulence model has been used to compute the flow pattern inside the diffuser system. The numerical simulations of the above mentioned equations are carried out until the residues fall below 1.0×10^{-6} for all the flow variables. To investigate the sensitivity of the grid in the axial and radial directions, a numerical investigation is performed for various grid sizes of 120×60 , 160×60 , 120×80 , and 180×50 . The present numerical simulations were carried out on 120×80 . The value of viscous sub-layer is kept above 26. Thus, the first computational grid is in the buffer layer of the turbulent boundary layer. The grid independent tests are carried out for the nozzles in the publications (Mehta *et al.* 2012).

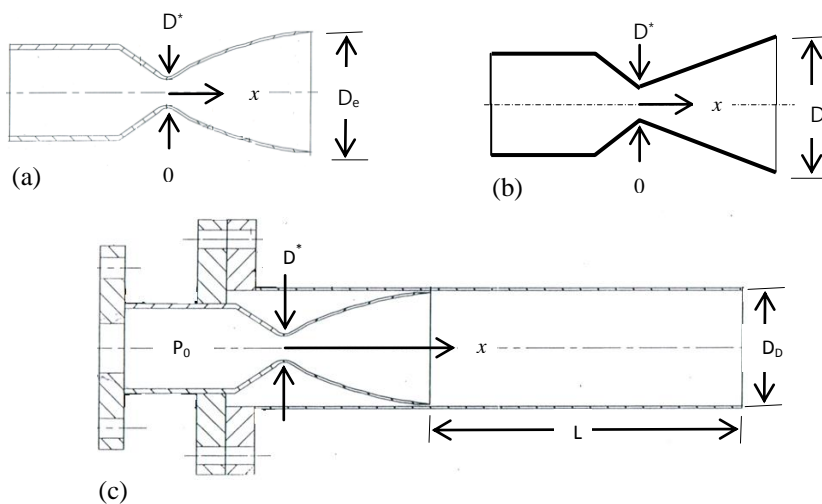


Fig. 1 Geometrical detail of contour (a), conical (b), and straight supersonic diffuser (c)

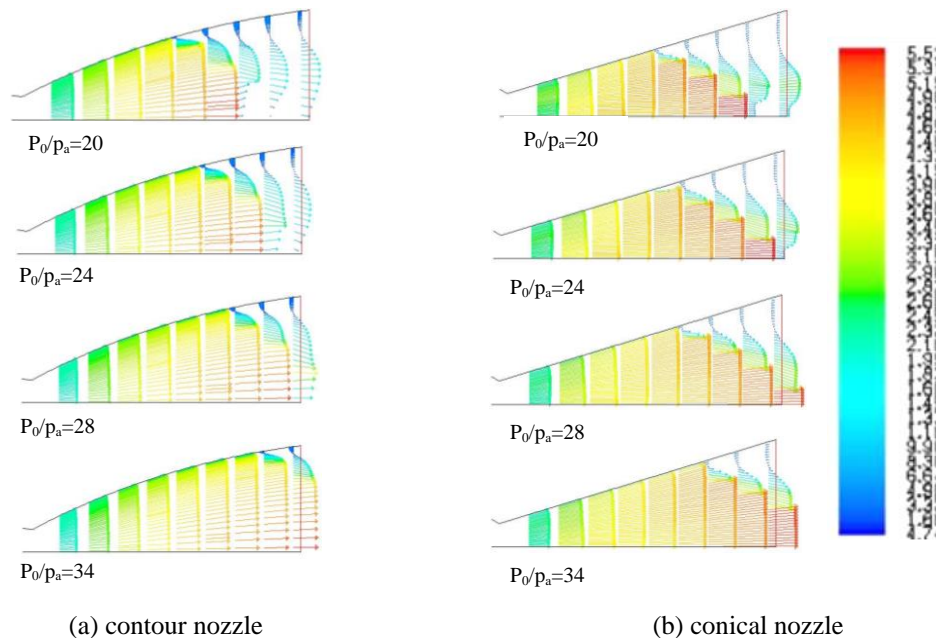


Fig. 2 Vector plots inside contour and conical nozzle

5. Results and discussion

5.1 Flowfield characteristics inside the contour and conical nozzle

Fig. 2 displays the vector plots for the contour and the conical nozzle. The colour bar is identical for all the vector and Mach contour plots. The vector plots are having different velocity profile at the identical stagnation to ambient pressure ratio P_0/p_a as depicted in Fig. 2. It can be seen from the velocity vector plots that the flow separation depends on the nozzle geometry for a given P_0/p_a . A large flow separation is noticed in the conical nozzle as compared to contour nozzle at $P_0/p_a=34$. Fig. 3 depicts the Mach contours for the contour and the conical nozzles for various value of P_0/p_a for 20 to 34. The Mach contour plots show that the shock wave location and shape depends on the nozzle geometry. The contour plots of the contour and conical nozzle indicate that the flow separation and shock wave inside the nozzle depend on the nozzle. It can be seen from Figs. 2 and 3 that the streamline depends on the nozzle geometry. The effects of geometry of the nozzle play significant role on the flowfield. A wall function approach (Saxena and Mehta 1986) is used to bridge the viscous sub-layer and the fully developed turbulent flow.

Fig. 4(a) and (b) depicts the variation of centerline and wall Mach number inside the contour nozzle. The Mach number value shown in Fig. 4 (b) is taken above the edge of the viscous sub-layer (Saxena and Mehta 1986). The centre line variations of Mach number and the value at the first grid from the wall of the contour and the conical nozzles are illustrated in Fig. 1. It is interesting to note that the formation of the hump in the conical nozzle is found between the axial locations of about 0.03-0.05 m as seen in Fig. 4(b). The two dimensional numerical simulation exhibits a hump in the centre line Mach number variation for the conical nozzle. This can be

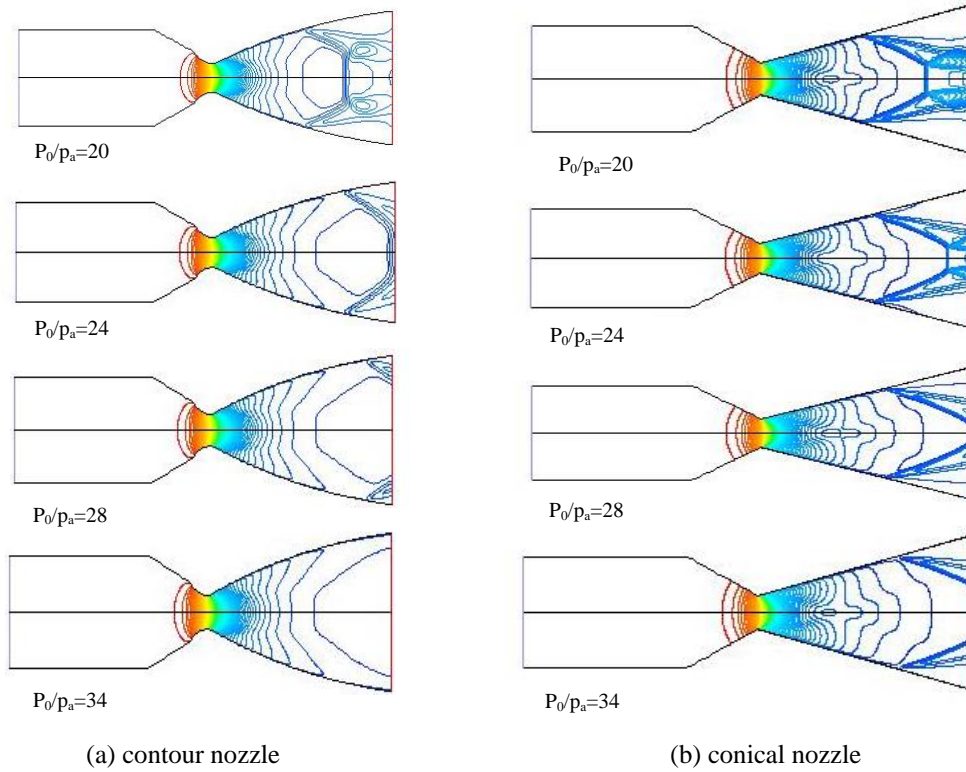


Fig. 3 Mach contour inside the contour and conical nozzle

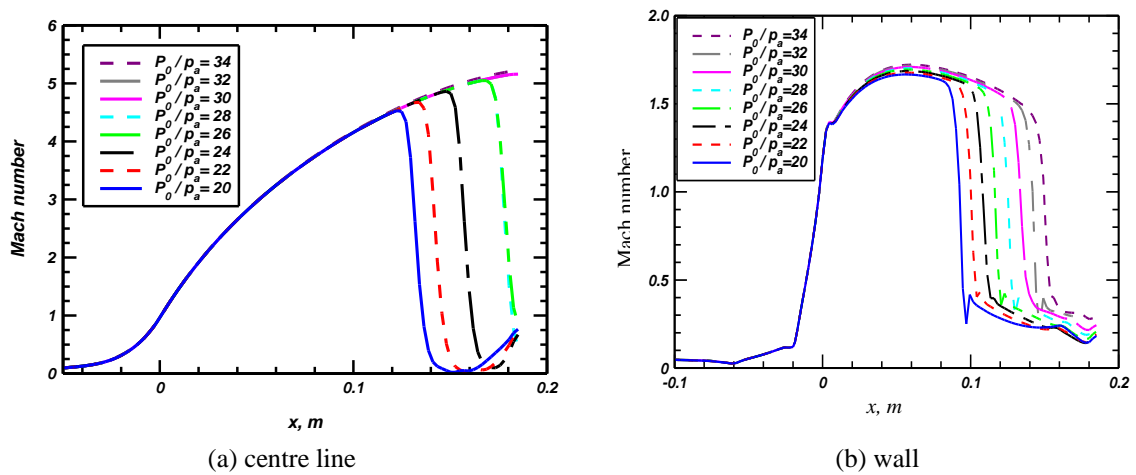


Fig. 4 Variation of centerline Mach number for various value of P_0/p_a for the contour nozzle

attributed to the geometrical parameters of the conical nozzle. The problem with small cone angles of the convergent-divergent conical nozzle is excessive nozzle length. The contour nozzle gives the minimum length of the nozzle with uniform flow at the nozzle exit. Any point of the flowfield

is described by two variables, the flow angle with respect to the centre line of the nozzle and the Prandtl-Meyer function (Liepmann and Roshko 2007). However, no hump formation is observed in the Mach profile of the contour nozzle. The distribution of the Mach number along the wall is influenced by the profile of the nozzle wall and the viscous effects. The average exit Mach number is higher in the contour nozzle as compared to the conical nozzle.

Fig. 5 (a) and (b) shows the variation of Mach number along the centre line and wall of the conical nozzle for various value of P_0/p_a respectively. The centerline maximum Mach number is 4.5. The wall maximum Mach number is 1.8. It shows the shock is moving towards the exit of the nozzle as the pressure ratio P_0/p_a increases. For a $P_0/p_a=28$, the normal shock goes out of the nozzle. All the normal shocks are located between 0.14 m to 0.185 m of the nozzle. Fig. 5 (b) shows formation of hump inside the conical nozzle. The flow behavior in the conical and the contour nozzles can be explained using quasi-one-dimensional isentropic flow which gives the relationship between the Mach number and the area ratio of conical nozzle.

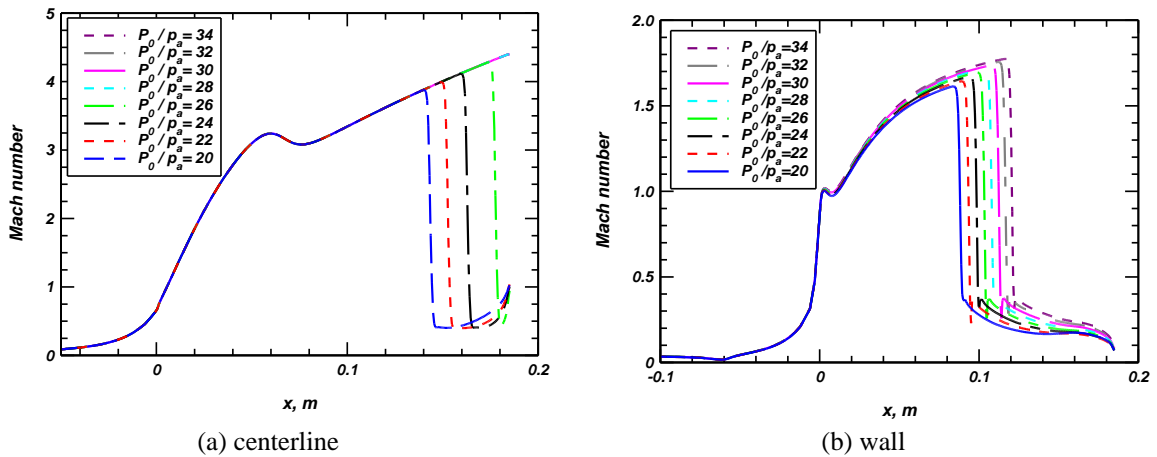


Fig. 5 Variation of Mach number for various value of P_0/p_a for conical nozzle

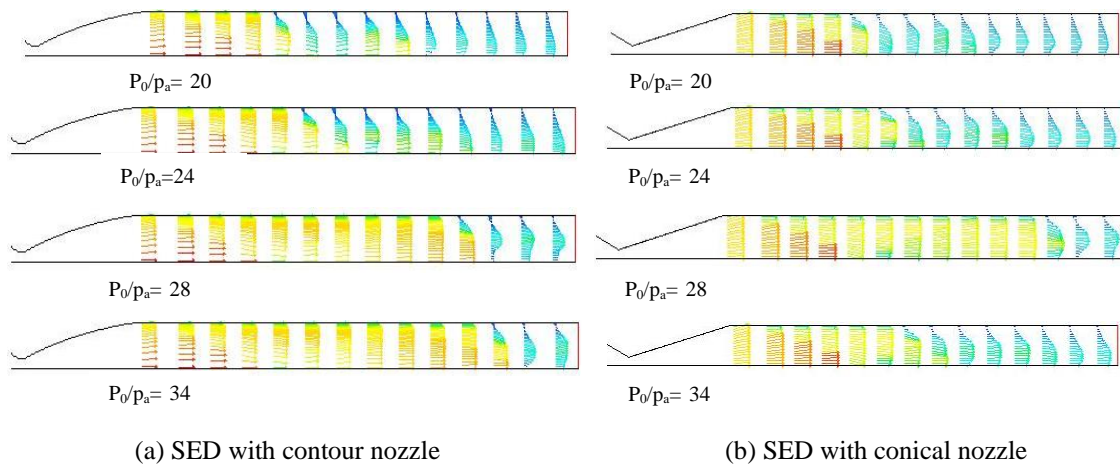


Fig. 6 Mach contour inside the contour and conical nozzle with SED

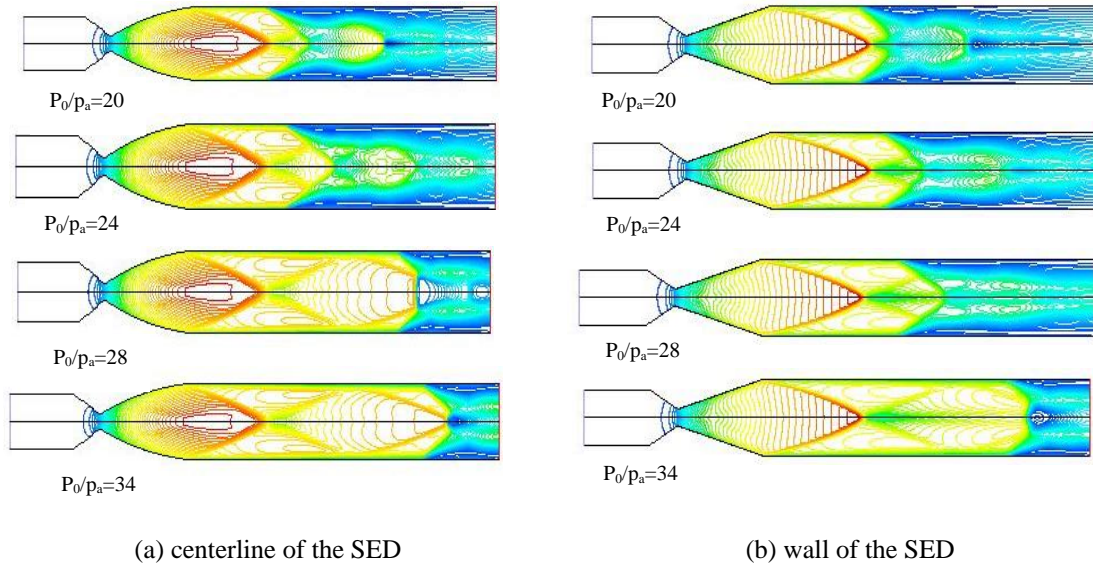


Fig. 7 Variation of Mach number along the wall of the SED (conical nozzle)

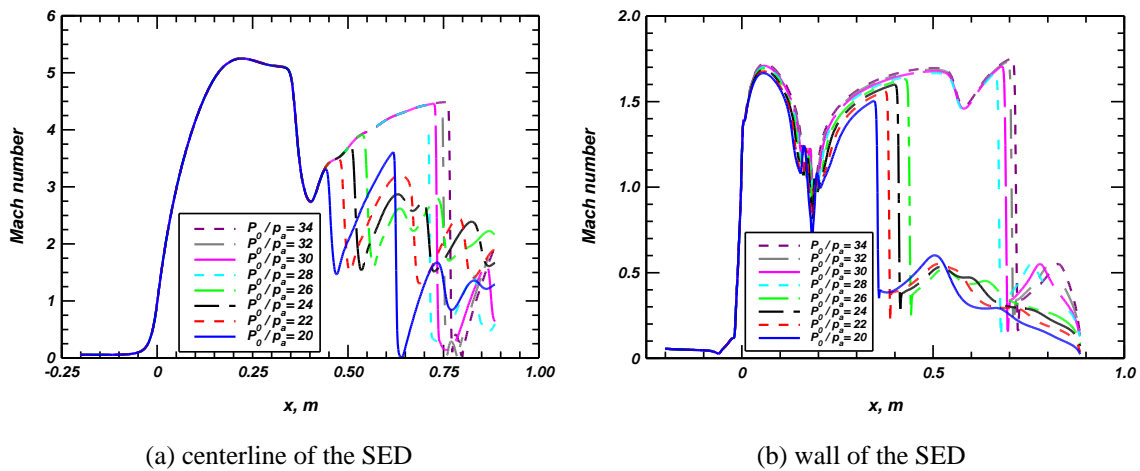
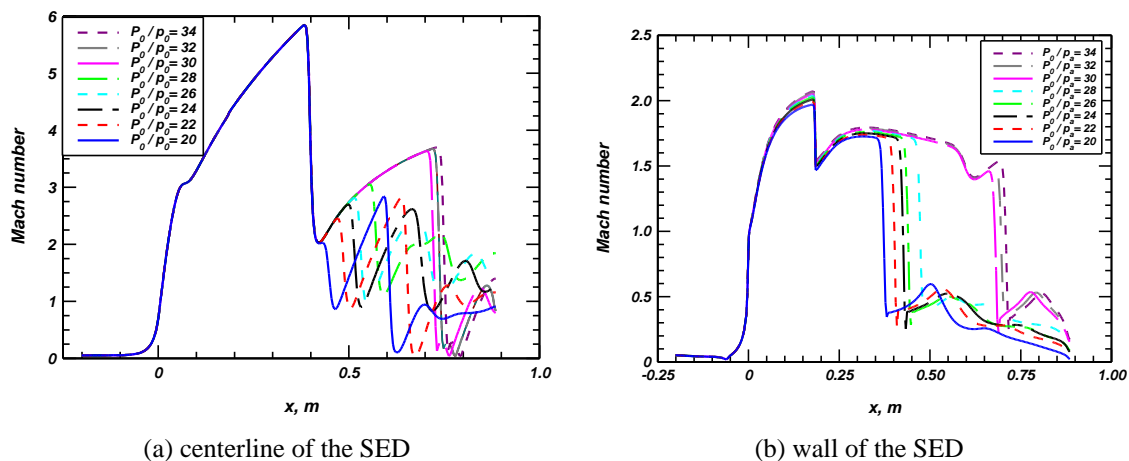


Fig. 8 Variation of Mach number along the SED (contour nozzle)

5.2 Flowfield characteristics inside the SED

The location of the shock structure was investigated with the different pressure ratios P_0/p_a of the diffuser. The normal shock wave, the oblique shock wave location, the flow separation behavior, and shear layer are analyzed. The diffuser diameter is the same as that of the nozzle exit diameter. The velocity vector profiles differ inside the SED and depend on the nozzle.

Fig. 6 (a) and (b) shows the vector plots inside the SED with contour and conical nozzles. Fig. 7(a) and (b) depicts the Mach contour plots inside the SED with contour and conical nozzles. It can be observed from the vector and Mach contour plots that the flowfield pattern inside the SED



(a) centerline of the SED (b) wall of the SED
 Fig. 9 Variation of Mach number along the wall of the SED (conical nozzle)

depends on the nozzle.

Fig. 8 (a) and (b) shows the variation of Mach number along the centerline and wall respectively for various values of P_0/p_a in the SED with the contour nozzle. The nozzle behaves like an under expanded nozzle. The maximum center line Mach number is 5.8. This indicates that the flow accelerates even after it exits from the nozzle. At a location of 0.4 m with a normal shock the flow turns subsonic. The maximum center line Mach number is 5.2. It clearly shows that there is a small increase in pressure as the flow comes out of the nozzle, unlike centerline pressure which continues to remain constant. The wall static pressure after a small increase continues to decrease before rising to the ambient pressure. Fig. 9 (a) and (b) shows the variation of Mach number along the centerline and wall respectively for various value of P_0/p_a in the SED with the contour nozzle. The variation of the centerline and wall Mach number differs with Fig. 8 (a) and (b). It reveals once again the flowfield as well as centerline and wall Mach number depend on the nozzle geometry.

5. Conclusions

Numerical simulation is performed to obtain the flowfield inside the contour and the conical nozzles (having identical area ratios) exhausting into a straight cylindrical SED by solving the axisymmetric time-dependent compressible turbulent Reynolds-Averaged Navier-Stokes equations. At the inlet of the nozzle stagnation-to ambient pressure ratio is varied from 20-34. The straight cylindrical SED is having $A_e/A^* = 21.7$ and $L/D = 5$.

A formation of a hump is observed in the centre line Mach number variation of the conical nozzle and is found to be a function of the geometrical parameters of the conical nozzle. The area ratio variations of the conical and the contour nozzles have significant influence on the gradient of Mach number. The contour nozzle gives uniform flow at the exit with the higher average Mach number as compared to the conical nozzle. The effects of geometry of the nozzle play significant role on the flowfield.

The contour and the conical nozzles display different flow characteristics. The maximum Mach

number along the centerline is higher for the contour nozzle than for the conical nozzle, where as the maximum Mach number along the wall displayed not much difference. These differences are attributed to the geometry of the nozzles. In the SED with conical nozzle, the conical nozzle behaves like an under expanded nozzle, where as the flow in the SED attached with contour nozzle showed fully expanded nozzle behavior.

Acknowledgments

Authors would like to thank Liquid Propulsion Systems Centre/Indian Space Research Organization for providing research grant under RESPOND project.

References

- Annamalai, K., Satyanarayan, T.N.V., Sriramulu, V. and Bhskaran, K.A. (2002), "Development of design methods for short cylindrical supersonic exhaust diffuser", *Exper. Fluid.*, **29**(2), 305-308.
- Delussu, G. and Talice, M. (2002), *Inviscid Supersonic Minimum Length Nozzle Design*, Centre for Advanced Studies, CRS4, Research and Development in Sardinia, Italy.
- Fluent 6.2 (2010), *Computational Fluid Dynamics Software User Guide*, Fluent Inc., Fluent India Pvt Ltd. Bangalore, India.
- Frey, M. and Hagemann, G. (2000), "Restricted shock separation in rocket nozzles", *J. Propuls. Pow.*, **16**(3), 478-484.
- Goethert, B.H. (1962), "High altitude and space simulation testing", *ARS J.*, **32**(6), 872-882.
- Kim, S. and Kwon, S. (2008), "Starting pressure and hysteresis behavior of an annular injection supersonic ejector", *AIAA J.*, **46**(5), 1039-1043.
- Kumaran, M.R., Vivekanadn, P.K., Sunderarajan, T., Kumaresan, K. and Raja Manohar, D. (2009), "Optimization of second throat ejectors for high-altitude test facility", *J. Propuls. Pow.*, **25** (3), 697-705.
- Liepmann, H.W. and Roshko, A. (2007), *Elements of Gas Dynamics*, First South Asian Edition, Dover Publications, Inc., New Delhi. India
- Massier, P.F. and Roschke, E.J. (1960), *Experimental investigation of exhaust diffusers for rocket engines, Progress in Astronautics and Rocketry: Liquid Rockets and Propellants*, Academic Press, NY, USA.
- Mehta, R.C., Natarajan, G. and Bose, N. (2012), "Fully expanded flow inside conical and contour nozzle", *J. Spacecraft Rock.*, **49**(2), 422-424.
- Park, B.H., Lee, J.H. and Yoon, W. (2008), "Studies on the starting transient of a straight cylindrical supersonic exhaust diffuser: effects of diffuser length and pre-evacuation state", *Int. J. Heat Fluid Flow*, **29**(10), 1369-1379.
- Park, B.H., Lim, J., Park, S., Lee, J.H. and Yoon, W. (2012), "Design and analysis of a second-throat exhaust diffuser for high altitude simulation", *J. Propuls. Pow.*, **28** (5), 1091-1104.
- Park, B.H., Lim, J.H., and Yoon, W. (2008), "Fluid dynamics in starting and terminating transients of zero-secondary flow ejector", *Int. J. Heat Fluid Flow*, **29**, 327-339.
- Saxena, S.K. and Mehta, R.C. (1986), "Shock/Turbulent boundary-layer interaction with wall function boundary conditions", *AIAA J.*, **24**(7), 1207-1209.
- Shapiro, A.H. (1953), *The Dynamics and Thermodynamics of Fluid Flow*, Vol. 1, Ronald Press, New York, USA.
- Sivo, J.N., Meyer, C.L. and Peters, D.J. (1960), *Experimental Evaluation of Rocket Exhaust Diffusers for Altitude Simulation*, NASA TN D-298, July.
- Spalart, P. and Allmaras, S.A. (1992), "One-equation turbulence model for aerodynamic flows", AIAA Ppaper 92-0439, Jan.

- Summerfield, M., Foster, C.R. and Swan, C.W. (1954), "Flow separation in overexpanded supersonic exhaust nozzles", *Jet Propuls.*, **24**(5) 319-321.
- Sung, H.G., Yeom, H.W., Yoon, S., Kim, S.J. and Kim, J. (2010), "Investigation of rocket exhaust diffusers for altitude simulation", *J. Propuls. Pow.*, **26**(2), 240-247.
- Yeom, H.W., Yoon, S. and Sung, H.G. (2009), "Flow dynamics at the minimum starting condition of a supersonic diffuser to simulate a rocket's high altitude performance on the ground", *J. Mech. Sci. Tech.*, **23**(2), 256-263.

EC